

A Rapid Extraction Method for Information on Complex Urban Land Cover Based on Oblique Photogrammetric Data

Cai Cai,^{1,2,3} Yingchun Tao,^{1,2,3} Xiya Zhang,⁴
Xiaojuan Xing,^{1,2,3} and Bogang Yang^{1,2,3*}

¹Beijing Institute of Surveying and Mapping, No. 15 Yangfangdian Road, Haidian District, Beijing 100038, China

²Beijing Key Laboratory of Urban Spatial Information Engineering, Beijing 100038, China

³Analysis and Application of Urban Big Data in Bogang Yang Staff Innovation Studio, Beijing 100038, China

⁴Institute of Urban Meteorology, China Meteorological Administration,
No. 55 Beiwaxili, Haidian District, Beijing 100089, China

(Received October 30, 2022; accepted January 23, 2023)

Keywords: rapid extraction, aerial photogrammetry, land cover, complex urban area, multi-level, orthophoto

With the development of sensors like digital aerial cameras and remote sensing and photogrammetry technologies, such as oblique photography and three-dimensional technology, higher resolution and richer data are available for urban land cover extraction, including digital orthophoto maps (DOMs), true digital orthophoto maps (TDOMs), and topographic information. On the basis of highly overlapped oblique photogrammetry, the output of TDOM can solve most of the occlusion problems caused by illumination and observation angles. Making full use of spatial information, especially height, may reduce spectral confusions among urban land covers due to limited spectral resolution in RGB images. We acquired and processed information from TDOM and height data based on aerial sensors and oblique photogrammetry and used a multi-level threshold method combining the vegetation color index, brightness, spatial information, and height to rapidly extract urban land cover information. The method offers a simple and effective way to automatically extract complex land cover information on megacities with no need for training sample selection. This method was evaluated by comparing its results from the area of Beijing with those from the most widely used support vector machine (SVM) and maximum likelihood classification methods through visual inspection and quantitative measures, and this method achieved a better accuracy.

1. Introduction

Urban land cover information and changes in it are of great importance to the urban ecological environment⁽¹⁾ and for urban planning and management.^(2,3) With the acquisition of a large number of high-resolution images from satellite and airborne sensors,⁽⁴⁾ the rich spatial information available provides a great opportunity for the automatic and efficient extraction of

*Corresponding author: e-mail: bogangy@126.com
<https://doi.org/10.18494/SAM4212>

urban land cover information and the changes in that information over time.⁽⁵⁾ The use of high-resolution images for urban land cover mapping and detection of changes has attracted widespread interest and is an area of intense research interest in the field of remote sensing.^(6–8)

Urban land cover information primarily includes the following categories: buildings, water bodies, vegetation (such as trees and grasslands), bare land, and impervious surfaces (e.g., roads, parking lots, and other paved areas). Buildings may contain different materials, be of different shapes, have different colors, and may even have green roofs covered by vegetation. Owing to the complexity of urban land cover types, for which large spectral differences between the same land cover types and the high spectral similarity of different land cover types are observed, spectral resolution from very high resolution (VHR) images (like RGB aerial images) is limited, and occlusion problems caused by illumination and observation angles arise.⁽⁸⁾ Thus, it can be difficult to accurately and automatically extract complex urban land cover information using only spectral information of VHR images^(9–11) To fully use the spatial information of VHR images, object-oriented classification methods and image texture assessments have been widely used.^(7–9) However, the problems of occlusion and confusion are still difficult to solve.

With the development of photogrammetry technologies, such as oblique photography and three-dimensional technology,⁽¹²⁾ digital orthophoto maps (DOMs), true digital orthophoto map (TDOMs), and topographic information such as digital surface models (DSMs) and digital elevation model (DEMs)⁽¹³⁾ can be obtained. By taking the height of objects into account, TDOM theoretically can completely correct geometric distortion and solve the problem of occlusion. TDOM has now proven to be a mature product and has been widely used⁽¹⁴⁾ in urban construction and management. In addition to reducing the problems of spectral confusion, the acquisition of DSMs and DEMs provides important supplementary information for the extraction of structures like buildings.^(1,5,11)

Supervised classification methods such as support vector machines (SVMs) have been widely applied to extract land cover information, but they cannot work without training samples. We acquired TDOM and height information and processed it based on aerial photogrammetry for urban land cover information extraction. After analyzing land cover characteristics in complex urban areas from photogrammetric data, we propose a multi-level threshold method to gradually extract different land cover categories based on the vegetation color index, brightness, spatial information, and height. This method offers a simple and effective way for the automatic extraction of complex land cover information in megacities.

2. Study Area

The study area was the central urban area of Beijing, China. This area is a fully urbanized area with the highest development intensity in the city of Beijing, which is very complex and contains diverse land covers, including areas with high buildings, low-rise cottage areas, green-roofs covered by vegetation, different colored roofs, water bodies, trees, grass, bare land, roads, parking lots, and other land covers.

3. Materials and Methods

We first used photogrammetric methods to obtain DSM, DEM, and TDOM data. Then by analyzing urban land cover characteristics, a method combining spectral and spatial information, especially height, we proposed to quickly extract the surface cover information of complex urban areas. Figure 1 shows the entire procedure of the proposed method.

Comprehensive response characteristics of typical urban land cover types in high-resolution aerial photogrammetric data were evaluated, including features of geometry, spectral data, texture, and height. Three types of information, i.e., height, vegetation color index, and height texture, could be easily and quickly obtained, even for the very high resolution images which contained large volumes of data. Because some buildings and trees had similar heights, it was difficult to obtain reliable building extraction results using height thresholds directly. To make full use of the spatial information in VHR images, the height was calculated using image segmentation and image texture methods to obtain the segmented object and height texture information. Then, we applied a multi-level threshold method by combining the vegetation color index, brightness, spatial information, and height and used it to extract water bodies, vegetation, buildings, pervious surfaces (e.g., bare land), and impervious surfaces. Finally, the results of each category were combined, and a result detailing the urban land cover information was generated.

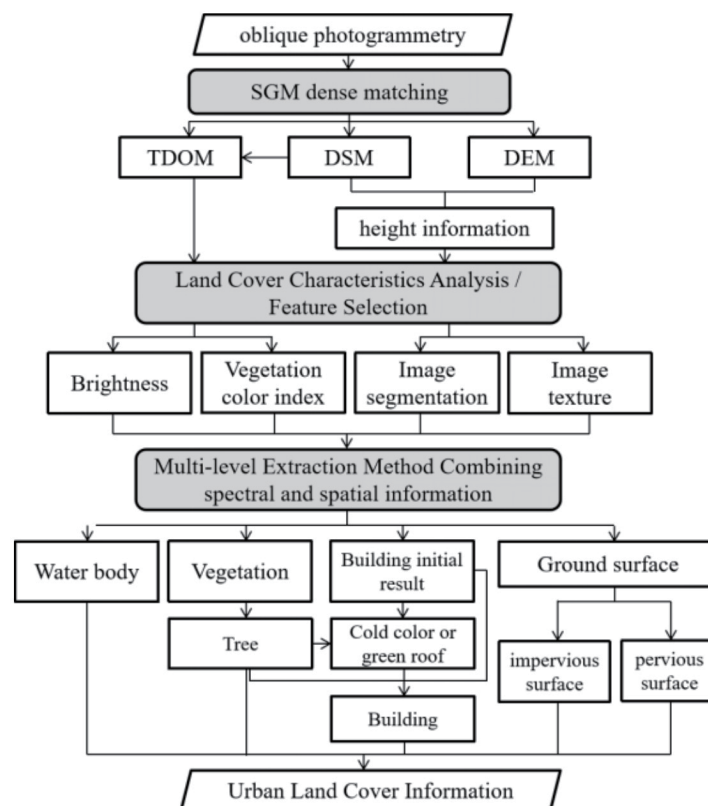


Fig. 1. Procedure of urban land cover information extraction described in this study.

3.1 TDOM and height information processing by aerial photogrammetry

Compared with a DOM, a TDOM is generally produced by replacing a DEM with a DSM. Digital differential correction technology is used to correct geometric distortions in the original image. After resampling the entire survey area, the visual angle of the image is corrected to the vertical visual angle. In practical applications, problems such as DSM acquisition and occlusion information compensation arise. A DSM can be obtained through dense matching or airborne laser detection and ranging (LiDAR) scanning, for which dense matching technology has become a popular method to obtain high-precision DSMs, which then may be used to solve problems of relative occlusion in multi-view image matching. The processing flow of TDOM and terrain data usually includes geometric corrections and joint adjustments of regional networks, multi-view image dense matching, DSM generation, and real orthophoto correction.

We acquired TDOM, DSM, and DEM data by the semi-global matching (SGM) method⁽¹⁵⁾ from aerial oblique photogrammetry. The TDOMs had three bands of red, green, and blue, with a spatial resolution of 0.5 m. It is worth noting that TDOM, DSM, and DEM data obtained by other sensors or methods, such as the use of unmanned aerial vehicles (UAVs), stereoscopic satellite data, high overlap aerial data, and height information based on LiDAR or even DOM were also used. Normalized DSM (nDSM), which represents height information, was obtained by calculating the difference between DSMs and DEMs. An nDSM reflects the true height of surface features after the topographic undulation factor is removed.

3.2 Feature selection

3.2.1 Vegetation color index

Vegetation indices [e.g., normalized vegetation index (NDVI)] have been proven fast and effective for the rapid and automatic extraction of large-area green coverage.⁽¹⁶⁾ However, because most geometrically corrected aerial photographs, UAV images, or processed satellite photographs only retain the three bands of red, green, and blue and lack the commonly used near-infrared bands, the vegetation color index was used in this study. Currently, the widely used vegetation color indices include the green leaf index (GLI),⁽¹⁷⁾ the normalized green-red difference index (NGRDI),⁽¹⁸⁾ the green chromatic coordinate (GCC), and the excess green minus excess red index (ExG-ExR).^(19–21)

Through the experimental comparison of these vegetation color indices including GLI, NGRDI, GCC, and ExG-ExR (Fig. 2), the difference between vegetation and non-vegetation [especially cool colored roofs shown in blue in Fig. 2(a)] was more significant in the GLI results [Fig. 2(b)], which are better for extracting vegetation. Therefore, the GLI was used in this study, the calculation of which is shown in Eq. (1):

$$GLI = (2G - R - B) / (2G + R + B), \quad (1)$$

where R , G , and B indicate the values of the red, green, and blue bands, respectively.

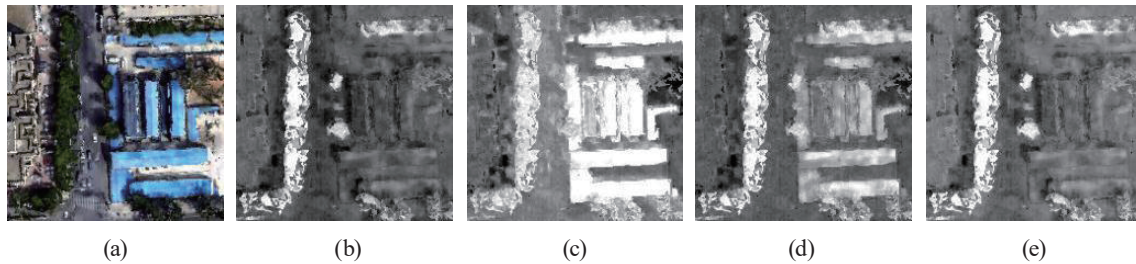


Fig. 2. (Color online) Part of TDOM of (a) the study area and (b)–(e) the comparison of the indices of the vegetation color results. The vegetation area has a higher index value, which appears bright, while the non-vegetation area has lower index value and appears dark. (a) TDOM. (b) GLI. (c) NGRDI. (d) ExG-ExR. (e) GCC.

A threshold of 0.1 for the GLI value was set to extract vegetation. If the index value was larger than 0.1, the area was classified as vegetation; otherwise, it was classified as non-vegetation.

3.2.2 Image segmentation method

Image segmentation is a prerequisite to object-based image analysis methods. The watershed transform-based image segmentation method has been commonly used; however, existing watershed transformation algorithms are very sensitive to noise and prone to produce over-segmentation. A region merging method has proven useful to optimize initial segmentation results.⁽²²⁾ We adopted a method based on watershed transformation and hierarchical region merging.⁽²²⁾ A multichannel watershed transformation method⁽²³⁾ was first used to produce an initial segmentation result. Neighboring segments with similar spectral features were then merged by comparing the average spectral vectors of neighboring segments to reduce the problem of over-segmentation. It is worth noting that other multiscale segmentation algorithms, such as the multiscale segmentation of e-Cognition software, are also suitable.

3.2.3 Image texture

Generally, different urban land cover types have different textural characteristics. For example, artificial land covers (e.g., buildings) generally vary evenly at the top of the ground features (except boundaries), while vegetation, especially trees, have many variations from the top, which appear more obvious in the texture. Therefore, image texture information can be used to assist land cover classification. We applied a widely used multivariate function to extract the texture of the height information, and the spectral angular distance was used for calculation. The minimum value of the texture in each direction was adopted to reduce the influence of the edge effect, which exists in omnidirectional textures.

3.2.4 Urban land cover characteristics

Comprehensive response characteristics of typical urban land cover types in VHR aerial images were studied, including features of the geometry, spectra, texture, and height. The height

information mainly highlights buildings and trees and can effectively reflect the difference between buildings and other impervious surfaces with the same spectral characteristics. The vegetation color index (e.g., GLI) can highlight areas of green vegetation. To diminish the confusion between green color roofs and trees, texture information can be helpful.

A part of the height, GLI, and height texture data from the study area is shown in Fig. 3. The different land cover types in this area can be clearly discerned. For example, most buildings have relatively high height values and low height texture data values; therefore, buildings show a reddish color in the false color composite map [Fig. 3(b)], and the boundaries are clear. With height information, buildings could be distinguished from other impervious surfaces (e.g., roads). Vegetation has relatively high GLI values, and the height of the grassland areas is normally low while trees have higher values. In addition, trees have relatively higher height texture data values than grasslands. Water bodies have relatively low heights and normally smooth textures. Because water bodies in urban areas have a high degree of eutrophication, they have relatively high GLI values [shown in green in Fig. 3(b)]. The impervious ground (e.g., roads) and pervious ground (e.g., bare soil) have similar low height data values and height texture data values. However, owing to urban management requirements, most bare land in the study area is covered with green mesh [Fig. 3(c)], which shows relatively high GLI values similar to grassland.

In addition, by comparing the image spectra of different types of land cover, we found that artificial land covers such as buildings and other impervious surfaces generally have relatively high band values (brightness), while natural land covers such as vegetation and water bodies generally have relatively low band values. Thus, the average value of all image bands was used as the brightness to characterize the comprehensive spectral reflectance, which is defined as BRI:

$$BRI = (R + G + B) / 3, \quad (2)$$

where R , G , and B indicate the values of the red, green, and blue bands, respectively.

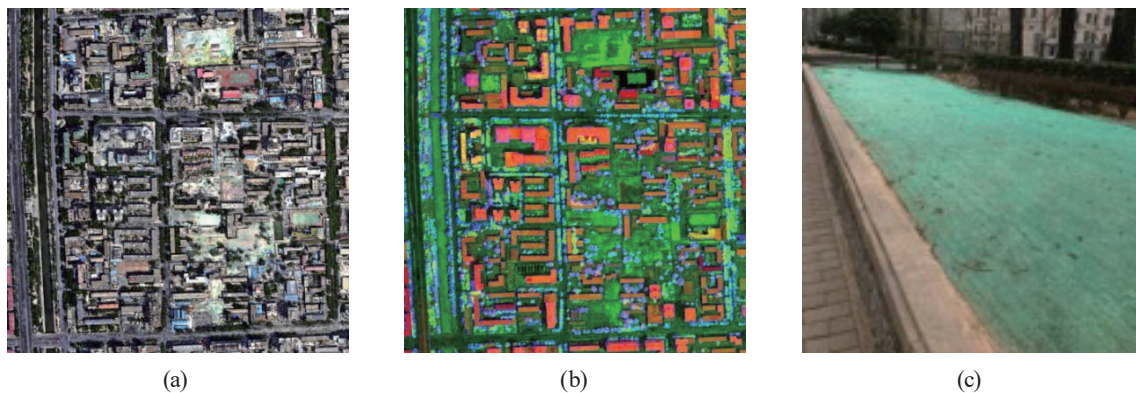


Fig. 3. (Color online) Urban land cover characteristics: (a) a part of a TDOM (resampled to 1 m), (b) false color composite map (R: height; G: GLI; B: height texture), and (c) an example of the green mesh covering on bare soil; the area shown is indicated by the red circle in (a).

3.3 Rapid extraction of urban land cover combining spectral and height information

By analyzing the characteristics of different land cover types, the vegetation color index that highlights information on the vegetation, the height data for distinguishing buildings, trees, and the ground surface, texture information for further classifying trees and buildings, and brightness information were generated. Image segmentation was then conducted in regards to height data to reduce height noise and make full use of the spatial information. According to height segments, the mean and mode values of height, GLI, and height texture were calculated for each object. A multi-level threshold method combining spectral and height information was used to extract water bodies, vegetation, buildings, pervious surfaces (e.g., bare land), and impervious surfaces.

(1) Water extraction method

As analyzed in Sect. 3.2.4, a body of water has relatively low height, height texture, and BRI values, along with certain GLI values. The thresholds of GLI, BRI, height, and height texture were generated and used to extract water bodies.

(2) Vegetation extraction method based on brightness correction

GLI can highlight vegetation information to a large extent, but owing to the lack of more effective near-infrared bands, some information on surfaces that are not vegetation would be confused with vegetation, such as some green roofs and green ground (e.g., fake turf) in cities. A cold-colored roof has a certain height, but its texture is relatively smooth, while trees have high texture values because of shadows and low BRI values as described in Sect. 3.2.4. Thus, a BRI threshold was generated to remove those mixed non-vegetation areas from the initial results of vegetation extraction from GLI. In addition, we set the height threshold to distinguish between trees and grasslands.

(3) Building extraction method based on a hierarchical strategy

We used a hierarchical strategy to gradually extract buildings, and subtle differences in the features of ground objects at different heights were fully utilized to select appropriate thresholds to obtain better results. Considering the spectral heterogeneity of VHR images, object-oriented and mode threshold methods were used for extraction. For each segmented height object, if a certain number of pixels were marked as a building, the object was classified as building.

The stratification and threshold values were selected according to the characteristics of buildings at different heights. Most ground can be eliminated by setting a threshold of a height of 2 m, because most buildings are higher than that. According to the features of buildings in the study area, three height layers were generated on the basis of the object-oriented average height data to extract buildings separately; the layers consisted of low-rise buildings (less than 2 floors), medium-height buildings (2–6 floors), and high-rise buildings (more than 6 floors). Because trees may have heights similar to low-rise buildings and to some medium-height buildings, trees were removed on the basis of previous results of vegetation extraction to obtain initial extraction results for buildings. However, some buildings with green roof gardens covered by vegetation may thereby be omitted. Generally, green roof gardens have relatively small variations in height, so the thresholds of height texture and the GLI of each object were carefully selected to separate trees and green roof gardens. Finally, the hierarchical extraction results were combined to obtain the final results of building extraction.

Other impervious surfaces and bare land were obtained by further threshold classification of the ground surface. By combining these results with the extraction results for water bodies, vegetation, and buildings, the final results of land cover information extraction result were obtained.

3.4 Methods of evaluating results

(1) Accuracy assessment

Buildings are the key type of land cover; therefore, building extraction and land cover extraction results were both visually and quantitatively evaluated. Widely used evaluation indicators including overall accuracy (OA), kappa coefficient, producer's accuracy (PA), and user's accuracy (UA) were adopted in this study.

According to the existing data, for the assessment of the accuracy of building extraction, a reference map of buildings that were manually collected from a 3D mesh model was used along with 800 testing samples selected by a stratified random method for the quantitative evaluation of land cover extraction.

(2) Comparison of results

To further verify the accuracy of the proposed method, we applied widely used methods for comparison, including the direct threshold method, the SVM classification method, and the maximum likelihood classification method. All methods were applied to the four-band images formed by the fusion of TDOM and height information. The training samples used in the SVM method and the maximum likelihood method were the same, and the testing samples used in all methods were the same.

4. Results and Discussion

4.1 Building extraction results and comparative validation

The results of building extraction using different methods are shown in Fig. 4. Compared with the reference map of buildings [Fig. 4(b)], our method [Fig. 4(c)] extracted most buildings, and the building patches were smooth and relatively complete. Green roof gardens and cold-colored roofs were extracted appropriately. The result using the direct threshold method [Fig. 4(d)], which is directly using thresholds of height and GLI, shows salt and pepper noise, and more misclassifications were made. The SVM results show less noise, were smoother, and had fewer misclassifications, but some omissions were still noted. The results of the maximum likelihood classification method showed some noise and some misclassifications, but they were better than the results of the direct threshold method.

Table 1 shows the results of the accuracy of the building extraction carried out using different methods. The overall accuracy and the kappa coefficient, which are 91.76% and 0.79, respectively, are both the highest for the results of the method proposed herein.

It is worth noting that both the SVM method and the maximum likelihood method require the manual collection of a large number of samples; thus, the manual workload is large, while the



Fig. 4. (Color online) Building extraction results (in purple) using different methods. (a) Part of the TDOM (resampled to 1m). (b) Building reference. (c) Extraction result of the proposed method. (d) Extraction result of the threshold method. (e) SVM classification result. (f) Maximum likelihood classification result.

overall efficiency is lower than that of the proposed method. In summary, the evaluation of the results shows that, compared with other methods, the proposed method can achieve higher accuracy in building extraction.

Table 1
Comparison of the accuracy of building extraction by different methods.

	Overall accuracy (%)	Kappa coefficient	Building extraction	
			Producer's accuracy (%)	User's accuracy (%)
Result of the proposed method	91.76	0.79	85.64	84.45
Result of the threshold method	87.69	0.71	88.32	72.61
SVM classification result	89.19	0.70	65.80	92.48
Maximum likelihood classification result	89.83	0.75	82.08	80.98

4.2 Results and comparative evaluation of urban land cover information extraction

The results of land cover extraction by different methods are shown in Fig. 5. To further verify the accuracy of the proposed method, we compared the extraction results with the

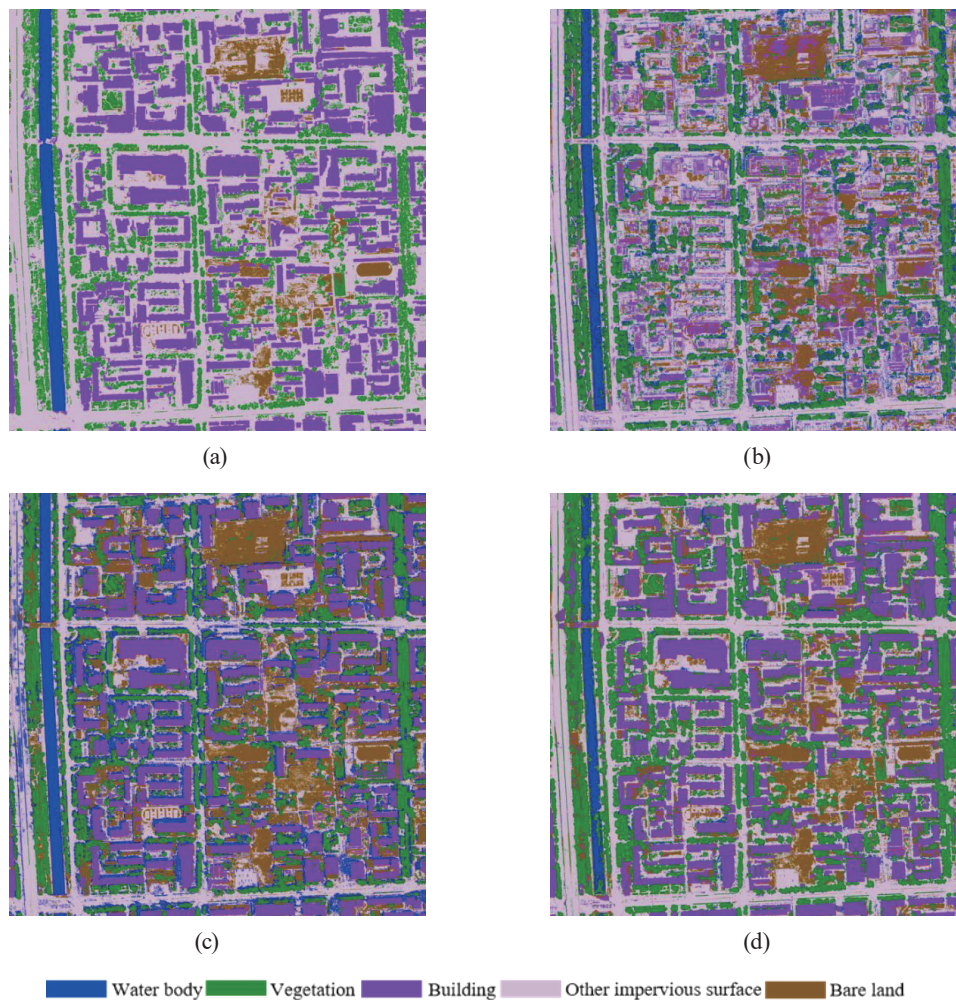


Fig. 5. (Color online) Extraction results of urban land cover information using different methods. (a) Extraction result of the proposed method. (b) Maximum likelihood classification result (spectral image only). (c) SVM classification result (spectral and height data). (d) Maximum likelihood classification result (spectral and height data).

maximum likelihood classifications based on spectral images alone [Fig. 5(b)], as well as the SVM classification [Fig. 5(c)] and maximum likelihood classification [Fig. 5(d)] based on the fusion of spectral information and height information. The training samples used in the SVM method and the maximum likelihood method were the same, and the testing samples used in all methods were identical.

Visually, the result of the proposed method [Fig. 5(a)] shows fewer classification errors, and the appearances of different land cover types are relatively complete and smooth. The rest of the results show water-related misclassifications, which are due to shadows, especially in the results of SVM classifications. The results based on the maximum likelihood classification of four-band images based on spectral information and height information also show a salt and pepper pattern, and some misclassifications occurred. Bare land extraction results by all methods are not as good, because those classifications have always been a difficult problem, even with more spectral bands.

Table 2 shows the accuracy of the extraction of land cover information by different methods. The accuracy of the proposed method is 84.99%, and the kappa coefficient is 0.81. The extraction accuracies for water, vegetation, and buildings are relatively high, which is consistent with the results of visual evaluations. For height information, the extraction accuracy is improved in

Table 2
Comparison of the land cover information extraction accuracy by different methods.

		Results from the proposed method	Maximum likelihood classification results (spectral images only)	SVM classification results (spectral and height)	Maximum likelihood classification results (spectral and height)
Buildings	Producer's accuracy (%)	91.47	36.68	80.84	93.39
	User's accuracy (%)	93.83	62.58	99.62	92.84
Water bodies	Producer's accuracy (%)	99.99	84.35	98.24	57.46
	User's accuracy (%)	100.00	91.29	76.85	94.25
Vegetation	Producer's accuracy (%)	86.92	93.32	94.25	98.41
	User's accuracy (%)	99.13	72.84	96.79	53.91
Other impervious surfaces	Producer's accuracy (%)	96.70	79.79	62.17	78.81
	User's accuracy (%)	61.67	58.65	80.92	83.83
Bare land	Producer's accuracy (%)	41.33	57.36	81.95	78.44
	User's accuracy (%)	96.73	46.20	61.57	76.40
Overall accuracy		84.99	64.32	81.77	81.20
Kappa coefficient		0.81	0.55	0.77	0.76

Note: The buildings herein were evaluated with other land cover types by testing samples, rather than by the building reference map shown in Sect. 4.1; therefore, the accuracy values are different from those in Table 1.

comparison with the result from the maximum likelihood classification method using spectral images only and that using spectral and height data.

In summary, from the perspective of visual evaluation and accuracy assessment, the proposed method can effectively extract land cover information in complex urban areas, especially for buildings, vegetation, and water bodies. The extraction of information on urban bare land has always been a difficult problem, even when more spectral bands are used in the analysis. Height information proved quite useful for land cover information extraction in complex urban areas.

5. Conclusions

Realizing the issues of low spectral resolution, ultrahigh spatial resolution, large amounts of data, no geometric distortion and displacement, little occlusion, and the ability to obtain topographic data at the same time as urban aerial remote sensing imagery, we studied a rapid extraction method of land cover information in complex urban areas by combining spectral and spatial data and height information. Using a comprehensive analysis of typical land cover characteristics, height, vegetation color index, height texture, and brightness, we developed a multi-level threshold method. Incorporating visual observations and accuracy evaluations of the experimental results as well as comparisons with the direct threshold method, SVM classification, and the maximum likelihood classification, we established the effectiveness of the method proposed. Without requiring the selection of training samples, the method offers a simple and efficient procedure for the automatic extraction of complex land cover information in megacities. This method is also applicable to other images from satellite and airborne sensors, such as UAV images, satellite images, and LiDAR data.

It is worth noting that with the development of photogrammetry and remote sensing pixel-level matching technology, especially with the engineering application of SGM technology, and through connection point matching, aerial triangulation, image control point measurements, and SGM matching of traditional digital aerial and satellite images, pixel level DSM and TDOM results with accuracy as high as those from oblique photogrammetry were obtained. Hence, the method described in this study has prospects for broad applications.

Acknowledgments

This study was funded by Beijing Key Laboratory of Urban Spatial Information Engineering, No. 2020204.

References

- 1 W. L. Stefanov, M. S. Ramsey, and P. R. Christensen: *Remote Sens. Environ.* **77** (2015) 173. [https://doi.org/10.1016/s0034-4257\(01\)00204-8](https://doi.org/10.1016/s0034-4257(01)00204-8)
- 2 Q. Weng: *Remote Sens. Environ.* **117** (2012) 34. <https://doi.org/10.1016/j.rse.2011.02.030>
- 3 S. J. Goetz, R. K. Wright, A. J. Smith, E. Zinecker, and E. Schaub: *Remote Sens. Environ.* **88** (2003) 1. <https://doi.org/10.1016/j.rse.2003.07.010>
- 4 *Multispectral Satellite Image Understanding*, C. Ünsalan, K. L. Boyer, Eds. (Springer-Verlag London, London, 2011) 1st ed., pp. 7–15. https://doi.org/10.1007/978-0-85729-667-2_2

- 5 X. Huang, Y. Wang, J. Li, X. Chang, Y. Cao, J. Xie, and J. Gong: *Sci. Bull.* **65** (2020) 1039. <https://doi.org/10.1016/j.scib.2020.03.003>
- 6 X. Tong, S. Liu, and Q. Weng: *IEEE J. Sel. Top. Appl. Earth Obs. Remote Sens.* **2** (2009) 61. <https://doi.org/10.1109/jstars.2009.2028160>
- 7 P. Li, J. Guo, B. Song, and X. Xiao: *IEEE J. Sel. Top. Appl. Earth Obs. Remote Sens.* **4** (2011) 103. <https://doi.org/10.1109/jstars.2010.2074186>
- 8 C. Cai, P. Li, and H. Jin: *Photogramm. Eng. Remote Sens.* **82** (2016) 335. <https://doi.org/10.14358/pers.82.5.335>
- 9 J. Wang, A. Ma, Y. Zhong, Z. Zheng, and L. Zhang: *Remote Sens. Environ.* **277** (2022) 113058. <https://doi.org/10.1016/j.rse.2022.113058>
- 10 M. Awrangjeb, M. Ravanbakhsh, and C. S. Fraser: *ISPRS J. Photogramm. Remote Sens.* **65** (2010) 457. <https://doi.org/10.1016/j.isprsjprs.2010.06.001>
- 11 X. Wang, P. Li, S. Jiang, J. Liu, and B. Song: *Remote Sens. Land Resour.* **28** (2016) 106. <https://doi.org/10.6046/gtzyyg.2016.02.17>
- 12 L. Li, C. Cai, and L. Zhao: *Beijing Surv. Mapp.* **3** (2017) 88. <https://doi.org/10.19580/j.cnki.1007-3000.2017.03.023>
- 13 X. Hua, W. Jun, and Z. Peng: *J. Guilin Univ. Electron. Technol.* **37** (2017) 134. <https://doi.org/10.3969/j.issn.1673-808X.2017.02.010>
- 14 X. Mai, X. Lu, and B. Long: *Geomatics Spat. Inf. Technol.* **9** (2015) 60. <https://doi.org/10.3969/j.issn.1672-5867.2015.09.020>
- 15 H. Hirschmuller: *IEEE Trans. Pattern Anal. Mach. Intell.* **30** (2008) 328. <https://doi.org/10.1109/TPAMI.2007.1166>
- 16 C. Cai, Y. Tao, Y. Zhang, and A. Wu: *Beijing Surv. Mapp.* **4** (2018) 237 (in Chinese). <https://doi.org/10.19580/j.cnki.1007-3000.2018.04.003>
- 17 M. Louhaichi, M. Borman, and D. Johnson: *Geocarto Int.* **16** (2001) 65. <https://doi.org/10.1080/10106040108542184>
- 18 E. Hunt, M. Cavigelli, C. Daughtry, and J. McMurtry: *Precis. Agric.* **6** (2005) 359.
- 19 D. Woebbecke, G. Meyer, K. Von Bargen, and D. Mortensen: *Trans. ASAE* **38** (1995) 259.
- 20 G. Meyer and J. Neto: *Comput. Electron. Agric.* **63** (2008) 282. <https://doi.org/10.1016/j.compag.2008.03.009>
- 21 L. Ding, Q. Li, X. Du, Y. Tian, and C. Yuan: *Remote Sens. Land Resour.* **28** (2016) 78. <https://doi.org/10.6046/gtzyyg.2016.01.12>
- 22 C. Cai, P. Li, and J. Guo: *Proc. 2012 IEEE Int. Workshop on Earth Observation and Remote Sensing Applications* (2012). <https://doi.org/10.1109/EORSA.2012.6261186>
- 23 P. Li and X. Xiao: *Int. J. Remote Sens.* **28** (2007) 4429. <https://doi.org/10.1080/01431160601034910>

About the Authors



Cai Cai received her B.S. degree from Wuhan University in 2010 and her Ph.D. degree from Peking University, China, in 2016. From 2014 to 2015, she was a research scholar at Columbia University, USA. Since 2016, she has been working at the Beijing Institute of Surveying and Mapping and as a researcher at the Beijing Key Laboratory of Urban Spatial Information Engineering, and since 2018, she has been a senior engineer. Her research interests are in urban spatial analysis and urban remote sensing. (caicai361448336@126.com)



Yingchun Tao received her B.S. degree in 2004, M.S. degree in 2007, and Ph.D. degree in 2019 from Peking University, China. Since 2007, she has been working at the Beijing Institute of Surveying and Mapping and as a researcher at the Beijing Key Laboratory of Urban Spatial Information Engineering, and since 2018, she has been a professor-level senior engineer. Her research interest is in urban spatial analysis. (taoyc@bism.cn)



Xiya Zhang received her Ph.D. degree in 2015 from Peking University, China. From 2013 to 2014, she was a research scholar at Columbia University, USA. Since 2015, she has been working at the Institute of Urban Meteorology, China Meteorological Administration, and since 2017, she has been a senior engineer. Her research interests are in urban meteorological disaster risk and urban remote sensing. (xyazhang@ium.cn)



Xiaojuan Xing received her B.S. degree in 2012 and M.S. degree in 2015 from Beijing Forestry University, Beijing, China. Since 2015, she has been an engineer at the Beijing Institute of Surveying and Mapping. Her research interests are in urban planning, geographic information, and cartography. (hengbin2009@126.com)



Bogang Yang received his Ph.D. degree in 2006 from Beijing Forestry University, China, and was engaged in postdoctoral work at Peking University from 2007 to 2009. Since 1983, he has been working at the Beijing Institute of Surveying and Mapping, and since 2004 he has been a professor-level senior engineer. He is the Director of the Beijing Key Laboratory of Urban Spatial Information Engineering. His research interests are in surveying and mapping technologies, smart city construction, and urban spatial analysis. (bogangy@126.com)